A Figure of Merit for Simultaneous-Multi-Beam Transmit Antenna Arrays

Anton N. Atanasov
Integrated Circuit Design
University of Twente
The Netherlands
a.n.atanasov@utwente.nl

Mark S. Oude Alink
Integrated Circuit Design
University of Twente
The Netherlands
m.s.oudealink@utwente.nl

Frank E. van Vliet
Defence, Safety & Security
TNO
Integrated Circuit Design
University of Twente
The Netherlands
frank.vanvliet@tno.nl

2022 IEEE International Symposium on Phased Array Systems & Technology (PAST) | 978-1-6654-4166-7/22/$31.00 ©2022 IEEE | DOI: 10.1109/PAST49659.2022.9974975

***Abstract*—We present a simple and useful figure of merit (FoM) with which to evaluate the performance of simultaneous-multi-beam (SMB) transmit (TX) antenna arrays. The FoM builds upon the power-aperture product and effective isotropic radiated power for single-beam arrays and extends it to SMB arrays. The FoM is the product of radiated power, antenna aperture efficiency and the amplifiers power added efficiency. We compute the FoM for three different two-beam TX systems to highlight their differences. This will enable systematic comparison and proper system design for modern and future multi-beam radar and communications.**

***Index Terms*—antenna arrays, multi-beam, figure of merit, power-aperture product, effective isotropic radiated power, mutual coupling, interleaved arrays, compact arrays, intermodulation, 5G, power added efficiency**

I. INTRODUCTION

Antenna arrays which are capable of simultaneously transmitting (TX) multiple beams at closely spaced frequencies are a natural evolution of existing array architectures. Simultaneous-multi-beam (SMB) functionality is critical for next generation radar, satellite and cellular telecommunications systems. It allows for increased search and track capabilities, for increased off-loading in high-throughput satellite links and for increased communication capacity.

It is difficult to directly compare the performance of different SMB designs, as the functionality can be achieved using very different architectures, e.g. subarrays [1], densely interleaved arrays [2], and others [3]. Each implementation either enforces some loss of efficiency or restricts the number of beams in some way that the system can support and as of yet, there is no direct manner of comparing their performance. The nature of the multiple signals now affects the performance of the power amplifiers (PAs) and the array in different ways. As a consequence, a designer may miss key benefits that one design can offer over another.

In this work we present a useful figure of merit (FoM) with which to help a designer better compare the overall performance of different multi-beam TX architectures. In Section II we define the key characteristics of a general multi-beam architecture and how they interact with one another. In Section III we present the derivation of the FoM together with an example use case. Finally, we summarize our work in Section IV.

II. SIMULTANEOUS-MULTI-BEAM TRANSMITTER ARRAYS

The generalized architecture of a TX array is shown in Fig. 1. It consists of a signal generator, which generates and maintains the necessary signals and phase relations, a set of M PAs which deliver power to every antenna element, and an antenna array consisting of N antennas in some arrangement. The manner in which each component is implemented can vary greatly from one design to another, but the overall architecture is the same. For SMB operation to be possible, the architecture of a given array must be partitioned in some manner.

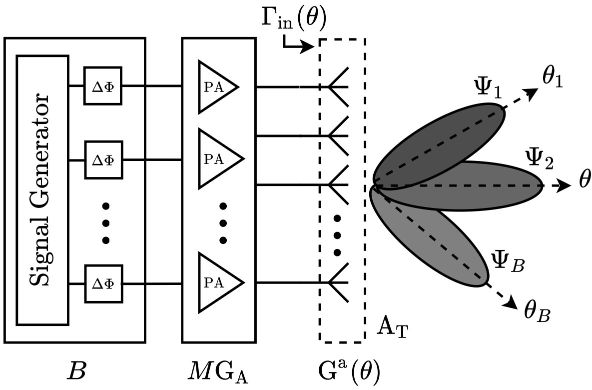

Fig. 1. Generalized simultaneous-multi-beam TX array architecture. The signal generator defines the signal properties, including the number of beams B. The amplification is done by M PAs with available gain G_A. The Antenna array consists of N antennas, with a total a physical aperture, A_T, and scan angle dependent active gain $\text{G}^\text{a}(\theta)$.

For example, in a digital beamforming system ($M = N$), each PA can be directly excited with several tones at different frequencies. This imposes a linearity constraint that may limit the PA's total output power as well as its efficiency due to AM/AM and AM/PM distortion in the form of intermodulation distortion (IMD). To reduce the effect of IMD, the PAs will need to operate in sufficient output backoff (OBO) and be subject to linearization techniques such as digital predistortion (DPD). Both approaches incur some penalty on the PA's

978-1-6654-4166-7/22/$31.00 ©2022 European Union

efficiency and heat budget [4], [5]. The IMD products must be sufficiently suppressed in order to comply with regulations on out-of-band emissions (adjacent channel leakage ratio (ACLR)) and in-band error vector magnitude (EVM) in the case of telecom applications. For radar applications, IMD products form beams which radiate in directions different from the main beams resulting in reduced performance [6], [7].

Alternatively, two or more single-beam subarrays can be spatially interwoven with each other or combined in blocks to create an SMB array [3], [8]. Most designs retain the $\lambda/2$ inter-element spacing, which means that the number of antennas per beam is reduced in order to fit within the array aperture boundaries of the design. As a consequence, the array active gain is reduced by a power of two. When spatially interleaving multiple subarrays, the relative spacing between the elements responsible for a given beam increases by multiples of $\lambda/2$, which leads to the emergence of grating lobes. Compact and superdirective arrays also offer SMB functionality and solve these issues, but they suffer from increased mutual coupling [9], [10].

Finally, antenna configurations can be built, which make use of an antenna's various radiation properties to create SMB operation without generating IMD within the PAs or strong mutual coupling between elements. Dual-polarized transmitter arrays are one such example, where two arrays, having orthogonal polarizations, are integrated into the same physical aperture [11]. Other designs may incorporate antennas which either operate outside of each other's bandwidths [12] or at different TE and TM modes [7]. The key aspect of all these approaches is to achieve "orthogonality" (minimal mutual coupling) in some dimension.

In short, an array design can compromise between physical aperture, active array gain, mutual coupling, scan angle and blindness, and other factors. Increasing the physical aperture of a multi-beam array to alleviate other design problems is seldom a feasible approach.

III. FIGURE OF MERIT DERIVATION

As SMB arrays can be designed with such a high degree of freedom, each design having its own strengths and weaknesses, there is a need for a FoM with which to compare different designs. For simplicity we consider a uniform linear array (ULA) with the same polarization for all beams, but the conclusions can be generalized to planar and volumetric arrays. The power-aperture product is a well-known FoM for estimating the total radiated power from an array [13]

$$\mathrm{P{\times}A} = \mathrm{P_t A_T}, \tag{1}$$

where $\mathrm{P_t}$ is the total transmitter power and $\mathrm{A_T}$ is usually the total antenna aperture. The design with the highest power-aperture product will achieve better range, detection and jammer burnthrough performance. The FoM does not take into consideration the antenna mutual coupling and the impact on the array gain and scan angle blindness. Finally, it assumes that all sources operate at the same frequency and are coherent, which is not the case for SMB operation where each beam radiates at a different frequency. For these reasons, the effective isotropic radiated power (EIRP) is a more convenient measure of how much power can be radiated from a given array structure in some direction θ, and the definition can be extended to describe SMB arrays. The EIRP is defined as

$$\mathrm{EIRP}(\theta) = \mathrm{P_t G^a}(\theta), \tag{2}$$

where $\mathrm{G^a}(\theta)$ is the array realized gain [14], when scanned to the angle θ. In the general context of transmission, increase in either $\mathrm{P_t}$ or $\mathrm{G^a}(\theta)$ can be directly related to an increase of the array's operational range. The goal of any SMB design is to achieve high EIRP and good efficiencies.

We first extend the definition of $\mathrm{P_t}$ for SMB operation. The active array gain, $\mathrm{G^a}(\theta)$, cannot be partitioned, because different beams are not coherent with one another as they operate at different frequencies. The total transmit power is partitioned between the number of beams, B, as

$$\mathrm{P_t} = \sum_{b=1}^{B} \mathrm{P}_b, \tag{3}$$

where P_b is the beam specific transmit power, which is dependent on the number of PAs allocated for a given beam as well as the necessary OBO to meet linearity constraints

$$\mathrm{P_b} = M_b \mathrm{G_A} \Delta_{\mathrm{OBO}} \mathrm{P_{in}}, \tag{4}$$

where M_b is the number of PAs for a given beam, $\mathrm{G_A}$ is the available gain of each PA at a given bias level (e.g. linear, $\mathrm{P_{1dB}}$, $\mathrm{P_{3dB}}$, etc.), Δ_{OBO} is the amount of OBO, and $\mathrm{P_{in}}$ is the PAs input power. Defining $\mathrm{P_b}$ in terms of $\mathrm{G_A}$ and Δ_{OBO} allows us to describe SMB designs that may either operate in compression (where they are more efficient) or need some OBO (less efficient) to meet a given linearity constraint. The choice of $\mathrm{G_A}$ instead of the more commonly used transducer gain, because the load mismatch due to mutual coupling is a function of the array realized gain.

Given the S-parameter matrix of an SMB array at the frequency of beam b and a beam-specific complex excitation coefficient with steering angle $a_{n,b}(\theta_b)$, the beam-specific active input reflection coefficient at the mth antenna is [15]

$$\Gamma_{m,b}(\theta_b) = \sum_{n=1}^{N} \mathrm{S}_{mn,b} a_{n,b}(\theta_b). \tag{5}$$

For an SMB design, the beam-specific array realized gain is then defined as [14]

$$\mathrm{G}_b^{\mathrm{a}}(\theta_b) = \frac{\mathrm{G_o}(\theta_b)}{N_b} \left(N_b^2 - \left| \sum_{n=1}^{N_b} \Gamma_{n,b}(\theta_b) \right|^2 \right), \tag{6}$$

where N_b is the number of antennas allocated per beam ($N_b \leq N$) and

$$\mathrm{G_o}(\theta) = \frac{4\pi}{\int_0^{\pi} F(\theta) \sin(\theta) d\theta} \eta_{\mathrm{rad}} \tag{7}$$

978-1-6654-4166-7/22/$31.00 ©2022 European Union

is the antenna element gain, with $F(\theta)$ being the magnitude of the radiation pattern and η_{rad} the antenna efficiency factor. Note that $\mathrm{G}_b^{\mathrm{a}}(\theta_b)$ is a function of N_b and $\Gamma_{n,b}(\theta_b)$ is a function of N because the mutual coupling is influenced by all antennas.

If the array is sufficiently large, then the majority of the antenna elements will experience approximately the same mutual coupling, such that $\Gamma_{n,b}(\theta_b) \approx \Gamma_b(\theta_b)$, leading to the following simplification

$$\mathrm{G}_b^{\mathrm{a}}(\theta_b) \approx N_b \mathrm{G}_{\mathrm{o}}(\theta_b)\left(1-|\Gamma_b(\theta_b)|^2\right). \tag{8}$$

Combining (4) and (8) and setting $N_b = M_b$, we define the EIRP of a beam given an SMB design and also fully account for the mutual coupling between all antennas

$$\mathrm{EIRP}_b(\theta_b) = N_b^2 \mathrm{G}_{\mathrm{o}}(\theta_b)(1-|\Gamma_b(\theta_b)|^2)\mathrm{G}_{\mathrm{A}}\Delta_{\mathrm{OBO}}\mathrm{P}_{\mathrm{in}}. \tag{9}$$

We define the SMB aperture efficiency per beam in a similar manner as [16]

$$\eta_{\mathrm{A}} = \frac{\left(\sum_{n=1}^{N_b} D_x D_y\right)^2}{N\sum_{n=1}^{N}\left(d_x d_y\right)^2} = \frac{\left(N_b D_x D_y\right)^2}{N^2\left(d_x d_y\right)^2} = \left(\frac{\mathrm{A}_b}{\mathrm{A}_{\mathrm{T}}}\right)^2, \tag{10}$$

where the denominator expression is the total antenna aperture, with $d_x d_y$ being the SMB array's unit cell, and the numerator expression is the array aperture for a beam, b, with a unit cell $D_x D_y$. This efficiency term penalizes the inefficient use of the entire aperture. This penalty can be though of as not achieving the maximum $\mathrm{EIRP}_b(\theta_b)$ for a given aperture constraint. When $\eta_{\mathrm{A}} = 1$, it means that the SMB's array aperture is fully utilized by all beams.

We define our FoM as the power-efficiency product of the sum of all $\mathrm{EIRP_b}$ of the SMB array, the aperture efficiency η_{A}, and the power added efficiency (PAE) of the PAs for each beam

$$\mathrm{FOM} \triangleq \sum_{\mathrm{b}=1}^{B}\left(\frac{\mathrm{A}_b}{\mathrm{A}_{\mathrm{T}}}\right)^2 \mathrm{EIRP_b\ PAE}. \tag{11}$$

We have omitted θ_b for clarity and evaluate EIRP_b at broadside instead. The summation over B accounts for the RF power delivered by all the PAs of the array. The FoM can be simplified by assuming that all beams have the same number of PAs and antennas, and that the mutual coupling effects are the same for each beam, giving

$$\mathrm{FOM} \triangleq \mathrm{B}\left(\frac{\mathrm{A}_b}{\mathrm{A}_{\mathrm{T}}}\right)^2 \mathrm{EIRP_b\ PAE}. \tag{12}$$

Thus, the FoM penalizes transmitters that have low efficiency, low PA gain, and it also penalizes multi-beam array designs which rely on physical separation between the subarrays. Conversely, the metric favours compact and efficient designs. For example, a system having high radiation efficiency but poor PA efficiency will be scored similarly to a system with poor radiation efficiency but high PA efficiency. The deciding factors would then become the total system gain and physical aperture.

A. Examples

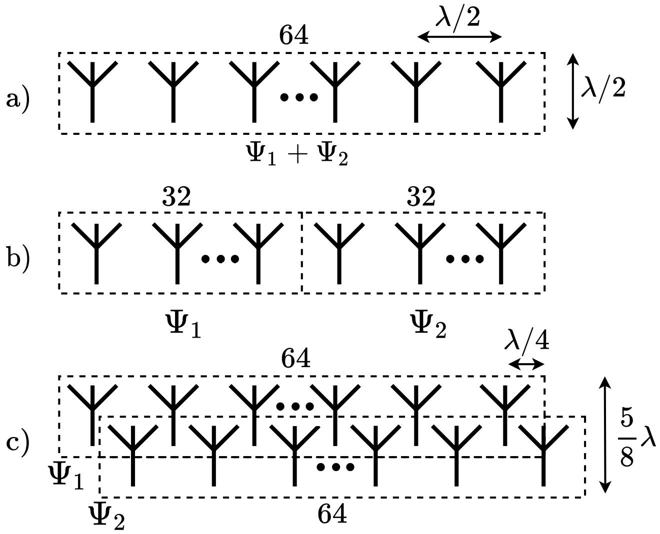

Fig. 2. Three distinct two-beam linear array architectures with $\lambda/2$ antenna spacing transmitting at frequencies Ψ_1 and Ψ_2, respectively. In a) the PAs operate at both frequencies with OBO, but all the elements are active. In b) the two single-beam arrays are placed next to each other and have only half the elements per beam. In c) the two arrays are densely interleaved with an offset of $\lambda/4$ by $\lambda/8$. In b) and c) each PA operates at a single frequency only.

Figure 2 shows three canonical examples of two-tone uniform linear dipole array (ULA) architectures, each achieving SMB operation in a different manner. All antenna elements and PAs are identical and equal in number. Similarly, the input power, $\mathrm{P_{in}}$, is kept constant across the three examples. All arrays are EM-simulated at two closely spaced frequencies Ψ_1 and Ψ_2, respectively. The first and second ULAs have 64 elements each with $\lambda/2$ element spacing. The third array consists of two identical 64 element ULAs with $\lambda/2$ element spacing, which are densely interleaved together with an offset of $\lambda/4$ by $\lambda/8$, resulting in a slight increase in the aperture area [2]. When the PAs operate at 6dB OBO, their available gain is $\mathrm{G_A} = 12\mathrm{dB}$ with a PAE of 35%. Correspondingly, when they operate at 0dB OBO, their $\mathrm{P_{sat}}$ gain is $\mathrm{G_A} = 11\mathrm{dB}$ with a maximum PAE of 55% [17].

The first array drives its PAs at both frequencies, allowing the number of antennas and the antenna aperture to remain unchanged. The aperture efficiency $\eta_{\mathrm{A}} = 1$ and the mutual coupling between the antenna elements at broadside is simulated to be $|\Gamma_b|^2 = 0.1$, where we have neglected the edge effects. The PAs have an available gain of $\mathrm{G_A} = 12\mathrm{dB}$, however due to the two tones, they must operate at 6dB OBO, which also reduces the efficiency of the PAs to 35%.

The second array consists of two subarrays having half the number of elements per tone as the previous array. While their PAs are also able to operate at a single tone each, their aperture

TABLE I
CALCULATION OF THE FOM FOR THE THREE EXAMPLE ARCHITECTURES.

Arrays	B [dB]	N_{b}^2 [dB]	$(A_{\mathrm{b}}/A_{\mathrm{T}})^2$ [dB]	G_0 [dBi]	$(1-\lvert\Gamma_{\mathrm{in}}\rvert^2)$ [dB]	G_{A} [dB]	Δ_{OBO} [dB]	PAE [dB]	**FOM [dB]**
a)	3	36.12	0	0	-0.46	12	-6	-4.56	**40.1**
b)	3	30.1	-6	0	-0.46	11	0	-2.6	**35.0**
c)	3	36.12	-1.94	0	-2.22	11	0	-2.6	**43.3**

efficiency is $\eta_{\mathrm{A}} = 0.25$. As the antenna elements are spaced $\lambda/2$ apart, their mutual coupling at broadside is identical to the first $|\Gamma_b|^2 = 0.1$. Similarly to the second array, the PAs can freely operate in compression and so their available gain is $\mathrm{G_A} = 11$dB with a PAE of 55%.

The third array consists of two densely interleaved arrays, which allow the PAs to operate at a single tone each at the expense of a slightly larger total antenna aperture and increased mutual coupling between the elements. The aperture efficiency is calculated to be $\eta_{\mathrm{A}} = 0.64$ and the mutual coupling between the antenna elements at broadside is simulated to be $|\Gamma_b|^2 = 0.4$. Since the PAs operate at a single tone each, they do not need any OBO and can operate further in compression, giving them an available gain of $\mathrm{G_A} = 11$dB with a PAE of 55%.

Each array has certain advantages and disadvantages over the others on the component level, which illustrates the new complexity that SMB arrays present. The evaluation of the FoM for the three arrays is summarized in Table I. All values converted to dB-scale for clarity. The first array has a score of 40.1dB, due to the high OBO and low PAE, despite having the highest $\mathrm{G_A}$ and η_{A}. This example highlights the importance of balancing the performance of the PAs and the array. The second array achieves the lowest score of 35.0 dB due to the reduced number of antenna elements per beam and poor η_{A}. It can maintain good PA performance and power, but the inefficient utilization of the available antenna aperture give it a very poor score. Finally, the densely interleaved array scores the highest with 43.3dB, because it mostly combines the benefits of the other two designs. It achieves good PA performance at the expense of higher mutual coupling and a decrease in η_{A}, which gives it an overall improvement of about 3.2dB over the first and most common design.

The FoM remains consistent in the two boundary cases when $B = 1$ and $B = N$, respectively. When $B = 1$ there is no multi-beam functionality so EIRP_b becomes the EIRP of the entire array with $N_b = N$. The performance of the first two arrays becomes identical with a FoM score of 44.0dB, as there is no need for OBO and all 64 antenna elements excite the same beam. The PAE and η_{A} of both arrays becomes 55% and 1, respectively. The $\mathrm{G_A}$ compresses to 11dB. The third array, on the other hand, now has 128 antenna elements exciting a single beam with the same PA conditions, giving it a FoM score of 48.3dB, which is still 4.3dB better than the other two designs.

When $B = N$, there is no beamforming as there are as many beams as there are antennas ($N_b = 1$), all radiating at different frequencies. The EIRP_b of every beam reduces to $\mathrm{G_o}(1 - |\Gamma_b|^2)\mathrm{G_A}\Delta_{\mathrm{OBO}}$ and the FoM is further penalized by $\eta_{\mathrm{A}} \sim 1/N^2$ and the PAs' PAE.

IV. CONCLUSION

This paper has presented a useful figure of merit with which to score the performance of a given simultaneous multi-beam transmitter array, regardless of its implementation. We consider the core components of a transmitter array to be a signal generation, a set of PAs and an array structure. The FoM is the product of the number of beams, the equivalent isotropic radiated power and the power added efficiency of a PA, normalized with respect to the total physical aperture of the system. The FoM penalizes designs with inefficient physical aperture per beam partitioning, relying on too much output power back-off, having low power added efficiency, or array gain. The FoM was applied to three two-beam TX array examples, each having specific advantages and disadvantages, that would be difficult to compare on a component level.

The FoM can aid designers to evaluate configurations where the maximum antenna aperture is limited, such as airborne platforms, and be used to optimize beams and power over the aperture. Alternatively, for configurations where the power consumption is limited, such as battery-operated equipment and handheld devices, it can be used to find a balance between area and power. Finally, in the general unconstrained case, it could be used to optimize SMB overall link budget.

REFERENCES

[1] H.-T. Chou, “Design Methodology for the Multi-Beam Phased Array of Antennas with Relatively Arbitrary Coverage Sector,” in *2017 11th European Conference on Antennas and Propagation (EUCAP)*, 2017, pp. 776–779.

[2] A. Atanasov, M. S. Oude Alink, and F. E. van Vliet, “Densely Interleaved Arrays for Dual-Tone Transmitters,” in *2019 IEEE International Symposium on Phased Array System Technology (PAST)*, 2019, pp. 1–6.

[3] R. J. Mailloux and S. G. Santarelli, “Mutual Coupling Effects and Their Compensation in a Time-Delay Scanned Array of Irregular Subarrays,” *IEEE Antennas and Wireless Propagation Letters*, vol. 12, pp. 657–660, 2013.

[4] S. Bhardwaj and J. Kitchen, “Broadband Parallel Doherty Power Amplifier in GaN for 5G Applications,” in *2019 IEEE Topical Conference on RF/Microwave Power Amplifiers for Radio and Wireless Applications (PAWR)*, 2019, pp. 1–3.

[5] K. Chaudhry, R. Quaglia, and S. Cripps, “A Load Modulated Balanced Amplifier with Linear Gain Response and Wide High-Efficiency Output Power Back-Off Region,” in *2020 International Workshop on Integrated Nonlinear Microwave and Millimetre-Wave Circuits (INMMiC)*, 2020, pp. 1–3.

[6] W. Sandrin, “Spatial Distribution of Intermodulation Products in Active Phased Array Antennas,” *IEEE Transactions on Antennas and Propagation*, vol. 21, no. 6, pp. 864–868, 1973.

[7] C. Hemmi, “Pattern Characteristics of Harmonic and Intermodulation Products in Broadband Active Transmit Arrays,” *IEEE Transactions on Antennas and Propagation*, vol. 50, no. 6, pp. 858–865, 2002.

[8] A. Hassanien and S. A. Vorobyov, “Phased-MIMO Radar: A Tradeoff Between Phased-Array and MIMO Radars,” *IEEE Transactions on Signal Processing*, vol. 58, no. 6, pp. 3137–3151, 2010.

[9] C. Volmer, J. Weber, R. Stephan, K. Blau, and M. A. Hein, “An Eigen-Analysis of Compact Antenna Arrays and Its Application to Port Decoupling,” *IEEE Transactions on Antennas and Propagation*, vol. 56, no. 2, pp. 360–370, 2008.

[10] C. Volmer, M. Sengul, J. Weber, R. Stephan, and M. A. Hein, “Broadband decoupling and matching of a superdirective two-port antenna array,” *IEEE Antennas and Wireless Propagation Letters*, vol. 7, pp. 613–616, 2008.

[11] F. Jia, S. Liao, and Q. Xue, “A Dual-Band Dual-Polarized Antenna Array Arrangement and Its Application for Base Station Antennas,” *IEEE Antennas and Wireless Propagation Letters*, vol. 19, no. 6, pp. 972–976, 2020.

[12] S.-Y. Chen and P. Hsu, “Broad-Band Radial Slot Antenna Fed by Coplanar Waveguide for Dual-Frequency Operation,” *IEEE Transactions on Antennas and Propagation*, vol. 53, no. 11, pp. 3448–3452, 2005.

[13] M. Skolnik, *Radar Handbook, Third Edition*, ser. Electronics electrical engineering. McGraw-Hill Education, 2008.

[14] R. Hansen, *Phased Array Antennas*, ser. Wiley Series in Microwave and Optical Engineering. Wiley, 1998.

[15] D. Pozar, “The Active Element Pattern,” *IEEE Transactions on Antennas and Propagation*, vol. 42, no. 8, pp. 1176–1178, 1994.

[16] G. D. Hopkins, J. Ratner, A. Traille, and V. Tripp, “Aperture Efficiency of Amplitude Weighting Distributions for Array Antennas,” in *2007 IEEE Aerospace Conference*, 2007, pp. 1–9.

[17] F. Raab, P. Asbeck, S. Cripps, P. Kenington, Z. Popovic, N. Pothecary, J. Sevic, and N. Sokal, “Power Amplifiers and Transmitters for RF and Microwave,” *IEEE Transactions on Microwave Theory and Techniques*, vol. 50, no. 3, pp. 814–826, 2002.

978-1-6654-4166-7/22/$31.00 ©2022 European Union